

## Measurements of the Rare Decay $K_L \rightarrow e^+e^-e^+e^-$

A. Alavi-Harati,<sup>12</sup> T. Alexopoulos,<sup>12</sup> M. Arenton,<sup>11</sup> K. Arisaka,<sup>2</sup> S. Averitte,<sup>10</sup> A. R. Barker,<sup>5</sup> L. Bellantoni,<sup>7</sup> A. Bellavance,<sup>9</sup> J. Belz,<sup>10</sup> R. Ben-David,<sup>7</sup> D. R. Bergman,<sup>10</sup> E. Blucher,<sup>4</sup> G. J. Bock,<sup>7</sup> C. Bown,<sup>4</sup> S. Bright,<sup>4</sup> E. Cheu,<sup>1</sup> S. Childress,<sup>7</sup> R. Coleman,<sup>7</sup> M. D. Corcoran,<sup>9</sup> G. Corti,<sup>11</sup> B. Cox,<sup>11</sup> M. B. Crisler,<sup>7</sup> A. R. Erwin,<sup>12</sup> R. Ford,<sup>7</sup> A. Glazov,<sup>4</sup> A. Golossanov,<sup>11</sup> G. Graham,<sup>4</sup> J. Graham,<sup>4</sup> K. Hagan,<sup>11</sup> E. Halkiadakis,<sup>10,\*</sup> J. Hamm,<sup>1</sup> K. Hanagaki,<sup>8</sup> S. Hidaka,<sup>8</sup> Y. B. Hsiung,<sup>7</sup> V. Jejer,<sup>11</sup> D. A. Jensen,<sup>7</sup> R. Kessler,<sup>4</sup> H. G. E. Kobrak,<sup>3</sup> J. LaDue,<sup>5</sup> A. Lath,<sup>10</sup> A. Ledovskoy,<sup>11</sup> P. L. McBride,<sup>7</sup> P. Mikelsons,<sup>5</sup> E. Monnier,<sup>4,†</sup> T. Nakaya,<sup>7</sup> K. S. Nelson,<sup>11</sup> H. Nguyen,<sup>7</sup> V. O'Dell,<sup>7</sup> M. Pang,<sup>7</sup> R. Pordes,<sup>7</sup> V. Prasad,<sup>4</sup> B. Quinn,<sup>4</sup> E. J. Ramberg,<sup>7</sup> R. E. Ray,<sup>7</sup> A. Roodman,<sup>4</sup> M. Sadamoto,<sup>8</sup> S. Schnetzer,<sup>10</sup> K. Senyo,<sup>8</sup> P. Shanahan,<sup>7</sup> P. S. Shawhan,<sup>4</sup> J. Shields,<sup>11</sup> W. Slater,<sup>2</sup> N. Solomey,<sup>4</sup> S. V. Somalwar,<sup>10</sup> R. L. Stone,<sup>10</sup> E. C. Swallow,<sup>4,6</sup> S. A. Taegar,<sup>1</sup> R. J. Tesarek,<sup>10</sup> G. B. Thomson,<sup>10</sup> P. A. Toale,<sup>5</sup> A. Tripathi,<sup>2</sup> R. Tschirhart,<sup>7</sup> S. E. Turner,<sup>2</sup> Y. W. Wah,<sup>4</sup> J. Wang,<sup>1</sup> H. B. White,<sup>7</sup> J. Whitmore,<sup>7</sup> B. Winstein,<sup>4</sup> R. Winston,<sup>4</sup> T. Yamanaka,<sup>8</sup> and E. D. Zimmerman<sup>4</sup>

(KTeV Collaboration)

<sup>1</sup>University of Arizona, Tucson, Arizona 85721

<sup>2</sup>University of California at Los Angeles, Los Angeles, California 90095

<sup>3</sup>University of California at San Diego, La Jolla, California 92093

<sup>4</sup>The Enrico Fermi Institute, The University of Chicago, Chicago, Illinois 60637

<sup>5</sup>University of Colorado, Boulder, Colorado 80309

<sup>6</sup>Elmhurst College, Elmhurst, Illinois 60126

<sup>7</sup>Fermi National Accelerator Laboratory, Batavia, Illinois 60510

<sup>8</sup>Osaka University, Toyonaka, Osaka 560-0043 Japan

<sup>9</sup>Rice University, Houston, Texas 77005

<sup>10</sup>Rutgers University, Piscataway, New Jersey 08854

<sup>11</sup>The Department of Physics and Institute of Nuclear and Particle Physics, University of Virginia, Charlottesville, Virginia 22901

<sup>12</sup>University of Wisconsin, Madison, Wisconsin 53706

(Received 5 February 2001)

We observe 441  $K_L \rightarrow e^+e^-e^+e^-$  candidate events with a background of 4.2 events and measure  $B(K_L \rightarrow e^+e^-e^+e^-) = [3.72 \pm 0.18(\text{stat}) \pm 0.23(\text{syst})] \times 10^{-8}$  in the KTeV/E799II experiment at Fermilab. Using the distribution of the angle between the planes of the  $e^+e^-$  pairs, we measure the  $CP$  parameters  $\beta_{CP} = -0.23 \pm 0.09(\text{stat}) \pm 0.02(\text{syst})$  and  $\gamma_{CP} = -0.09 \pm 0.09(\text{stat}) \pm 0.02(\text{syst})$ . We also present the first detailed study of the  $e^+e^-$  invariant mass spectrum in this decay mode.

DOI: 10.1103/PhysRevLett.86.5425

PACS numbers: 13.20.Eb, 11.30.Er, 13.40.Hq, 14.40.Aq

The rare decay  $K_L \rightarrow e^+e^-e^+e^-$  proceeds via a two-virtual-photon intermediate state with internal photon conversions to  $e^+e^-$  pairs. This permits a measurement of the  $K_L\gamma^*\gamma^*$  form factor, which is necessary to understand the long distance contributions to other rare  $K_L$  decays, in particular,  $K_L \rightarrow \mu^+\mu^-$  [1], whose short distance processes are sensitive to the Cabibbo-Kobayashi-Maskawa matrix element  $V_{td}$ . The QED prediction [2], neglecting radiative corrections and a form factor, for the ratio  $B(K_L \rightarrow e^+e^-e^+e^-)/B(K_L \rightarrow \gamma\gamma)$ , together with the experimental measurement of  $B(K_L \rightarrow \gamma\gamma)$  [3], gives a branching ratio of  $(3.65 \pm 0.09) \times 10^{-8}$ . The most precise previous measurements with  $K_L \rightarrow e^+e^-e^+e^-$  were based on 27 candidate events [4]. We report here a measurement of the branching ratio of the rare decay  $K_L \rightarrow e^+e^-e^+e^-$  at the Fermilab experiment E799II. We also present a study of  $CP$  symmetry in this decay and the first analysis of a  $K_L\gamma^*\gamma^*$  form factor.

The data were collected in 1997 with the KTeV detector at Fermilab. The detector components are described in [5,6]. During E799II running conditions, 800 GeV pro-

tons struck a BeO target; collimators and magnets defined two nearly parallel  $K_L$  beams, which decayed in a 65 m long region held under vacuum. The decay region was surrounded by photon veto detectors designed to detect particles escaping the fiducial volume of the detector. A charged particle spectrometer, consisting of four drift chambers and an analyzing magnet, was used to determine the charge, momentum, and trajectories of particles. A pure CsI calorimeter with 3100 crystals was used for photon detection and charged particle identification.

The four-track trigger used to collect this dataset is described in detail in [5]. In the off-line analysis, we require two positively charged tracks and two negatively charged tracks from a common vertex. At least three tracks must strike the CsI; the fourth may strike the CsI or pass through one of the CsI beam holes. A track is identified as an  $e^\pm$  if its  $E/P$ , the ratio of the energy measured by the calorimeter to the momentum measured by the charged spectrometer, is between 0.9 and 1.1. We require the energy of the clusters deposited in the calorimeter to be greater than 2 GeV. We also place cuts on the track and vertex quality

and require the photon veto energies to be no more than the level of typical accidental activity.

To select  $K_L \rightarrow e^+e^-e^+e^-$  events we require the decay vertex to be within the fiducial region of 95–155 m from the target and the total momentum of the kaon in the lab to be between 25–215 GeV/c. Figure 1 shows the distribution of the  $P_T^2$ , the square of the component of the total momentum of the daughter particles ( $e^+e^-e^+e^-$ ) transverse to the kaon line of flight, versus the four body invariant mass for the data sample and for a Monte Carlo simulation. We define the signal region by  $P_T^2$  less than 300 (MeV/c)<sup>2</sup> and  $|M_{e^+e^-e^+e^-} - M_{K^0}|$  less than 30 MeV/c<sup>2</sup>, with 90% efficiency. The liberal cut on  $M_{e^+e^-e^+e^-}$  was chosen to retain radiative events  $K_L \rightarrow e^+e^-e^+e^-(\gamma)$  with an undetected soft photon.

A source of background to  $K_L \rightarrow e^+e^-e^+e^-$  is  $K_L \rightarrow e^+e^-\gamma$  or  $K_L \rightarrow \gamma\gamma$ , with one or two photon conversions in the detector material. The photon conversion probability in the material upstream of the first drift chamber in our detector is  $(2.74 \pm 0.11) \times 10^{-3}$  [7]. Removing events that have a minimum track separation at the most upstream drift chamber of less than 1 mm reduces this background to  $3.7 \pm 0.3$  events, estimated from Monte Carlo. Another source of background

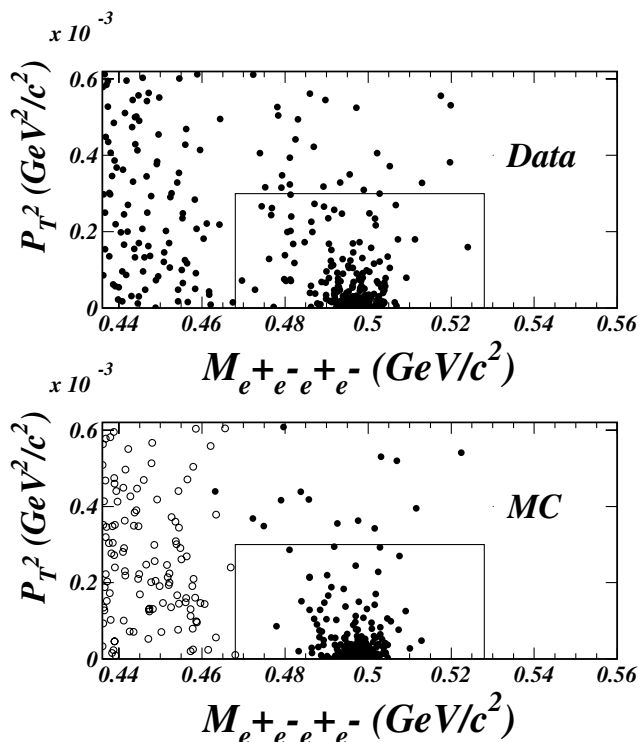


FIG. 1. Top: The distribution of  $P_T^2$  vs  $M_{e^+e^-e^+e^-}$  for candidate  $K_L \rightarrow e^+e^-e^+e^-$  events after all cuts except the  $P_T^2$  and  $M_{e^+e^-e^+e^-}$  cuts. There are 441 events in the signal region defined by the box. Bottom: The distribution of  $P_T^2$  vs  $M_{e^+e^-e^+e^-}$  for reconstructed Monte Carlo simulated events, scaled to the data statistics. The filled circles represent the signal Monte Carlo and the open circles represent the  $K_L \rightarrow \pi^\pm e^\mp \nu e^+e^-$  Monte Carlo. The box defines the signal region with an efficiency of 90%.

is  $K_L \rightarrow \pi^\pm e^\mp \nu e^+e^-$ , where the pion misses the calorimeter because of the beam holes and is incorrectly assumed to be an electron. The kinematic limit for the invariant mass with the pion misidentified as an electron is 478 MeV/c<sup>2</sup>. Since  $B(K_L \rightarrow \pi^\pm e^\mp \nu e^+e^-)$  is not measured, we estimate it from the branching ratio of the parent decay  $K_L \rightarrow \pi^\pm e^\mp \nu \gamma$ . This background is seen in the lower mass region in Fig. 1 (top) and is estimated to be  $0.5 \pm 0.5$  events. After all selection criteria are applied, we observe a total of 441  $K_L \rightarrow e^+e^-e^+e^-$  candidate events and estimate the total background to be 4.2 events, as described above. The distribution of the invariant mass of  $e^+e^-e^+e^-$  for the data and the Monte Carlo is shown in Fig. 2.

The distribution of the  $e^+e^-$  invariant masses in the  $K_L \rightarrow e^+e^-e^+e^-$  decay reveals the internal structure of the  $K_L \gamma^* \gamma^*$  vertex. A related decay,  $K_L \rightarrow e^+e^-\gamma$ , probes the  $K_L \gamma \gamma^*$  vertex; the form factor for that decay has been parametrized by Bergström, Massó, and Singer (BMS) [8,9],

$$f(x) = \frac{1}{1 - x(m_K^2/m_\rho^2)} + \frac{C\alpha_{K^*}}{1 - x(m_K^2/m_{K^*}^2)} \times \left[ \frac{4}{3} - \frac{1}{1 - x(m_K^2/m_\rho^2)} - \frac{1}{9[1 - x(m_K^2/m_\omega^2)]} - \frac{2}{9[1 - x(m_K^2/m_\phi^2)]} \right],$$

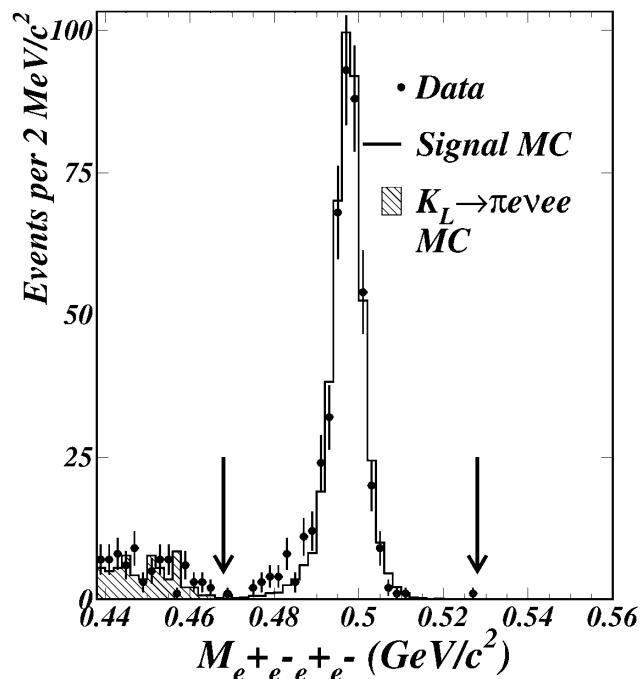


FIG. 2. The  $M_{e^+e^-e^+e^-}$  distribution after all cuts except the invariant mass cut. The dots represent the data and the histogram represents the Monte Carlo simulation. The arrows indicate an intentionally wide mass window chosen to retain the low-side radiative tail visible in the data. The decay  $K_L \rightarrow \pi^\pm e^\mp \nu e^+e^-$  is seen in the lower mass region.

where  $x \equiv M_{ee}^2/M_K^2$  and  $M_K, M_\rho, M_{K^*}, M_\omega,$  and  $M_\phi$  are the invariant masses of the corresponding mesons. The parameter  $\alpha_{K^*}$  describes the relative strength of an intermediate pseudoscalar decay amplitude and a vector meson decay amplitude. The constant  $C$  is determined using various coupling constants and is equal to 2.3 [8,9]. The BMS model predicts  $|\alpha_{K^*}| = 0.2\text{--}0.3$ ; note that  $\alpha_{K^*} \approx 0.3$ , rather than zero, best approximates a pointlike form factor [ $f(x) = 1$ ] for this analysis. Since there are two  $e^+e^-$  pairs in this decay, we use a factorized expression for the form factor.

We fit for the BMS parameter  $\alpha_{K^*}$  from our 441 event sample using a likelihood function as in [6,10] with one parameter. The likelihood function is based on the  $K_L \rightarrow e^+e^-e^+e^-$  matrix element which is a function of all kinematic variables. Our  $K_L \rightarrow e^+e^-e^+e^-$  Monte Carlo simulation uses the matrix element calculation found in [2] and does not include radiative corrections. Since radiative corrections could potentially have a large effect on the form factor measurement, in reality we measure an effective parameter,  $\alpha_{K^*}^{\text{eff}}$ , which takes into account both the radiative effects and the form factor. Using the likelihood function we obtain  $\alpha_{K^*}^{\text{eff}} = -0.14 \pm 0.16(\text{stat}) \pm 0.15(\text{syst})$ . Figure 3(a) shows the  $x$  distribution for data and for Monte Carlo using our measured form factor and using a pointlike form factor. The bin-by-bin ratios of data/Monte Carlo [Figs. 3(b) and 3(c)] further demonstrate the difference between our measured value of  $\alpha_{K^*}^{\text{eff}}$  and  $f(x) = 1$ . The systematic uncertainty of 0.15 is due to the detector

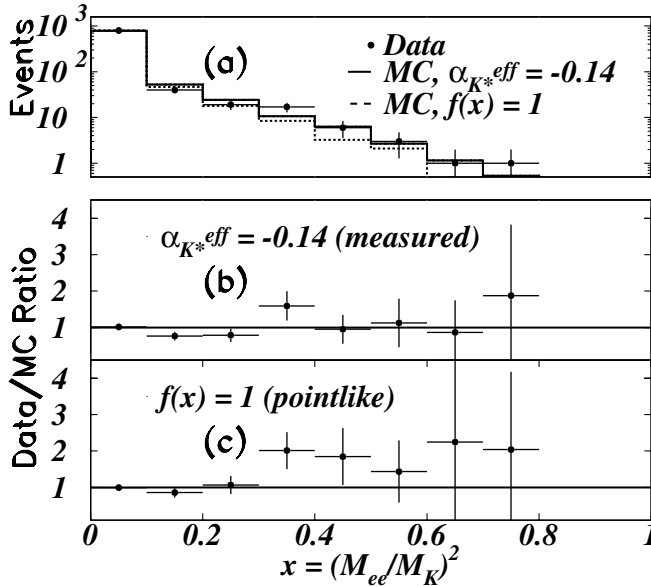


FIG. 3. (a) The  $x$  distribution for data and for Monte Carlo using our measured value of  $\alpha_{K^*}^{\text{eff}}$  and using  $f(x) = 1$ . Since there are two  $e^+e^-$  pairs in this decay, this is a double entry plot. The data/Monte Carlo ratio is shown for our measured value of  $\alpha_{K^*}^{\text{eff}}$  (b) and for a pointlike form factor (c). We measure  $\alpha_{K^*}^{\text{eff}} = -0.14 \pm 0.16(\text{stat}) \pm 0.15(\text{syst})$ . Recall that  $\alpha_{K^*} \approx 0.3$  best approximates a pointlike form factor.

acceptance and is dominated by the uncertainty in reconstruction of the  $Z$  position of the vertex and the calorimeter energy. Our result is in agreement with the recent measurement of  $\alpha_{K^*}^{\text{eff}} = -0.15 \pm 0.06(\text{stat}) \pm 0.02(\text{syst})$  for the decay  $K_L \rightarrow e^+e^-\gamma$  [11], also ignoring radiative corrections (including radiative corrections to  $K_L \rightarrow e^+e^-\gamma$ ,  $\alpha_{K^*} = -0.36 \pm 0.06(\text{stat}) \pm 0.02(\text{syst})$  [11]. The world average value for this decay mode is  $\alpha_{K^*} = -0.33 \pm 0.05$  [3]). Note that the effect of radiative corrections on  $\alpha_{K^*}$  could well be different in the two modes.

We also study the form factor parametrization of D'Ambrosio, Isidori, and Portolés (DIP) [12]. This parametrization of the  $K_L\gamma^*\gamma^*$  form factor is a function of two real coefficients of linear and quadratic terms ( $\alpha_{\text{DIP}}$  and  $\beta_{\text{DIP}}$ , respectively) and is relatively model independent. Using a factorization model [12] the expectations for  $\alpha_{\text{DIP}}$  and  $\beta_{\text{DIP}}$  from a  $\rho$  form factor are  $-1.2$  and  $1.4$ , respectively. Because of the dominance of low  $M_{ee}$ ,  $K_L \rightarrow e^+e^-e^+e^-$  is much less sensitive to the second order term ( $\beta_{\text{DIP}}$ ) than the decay  $K_L \rightarrow e^+e^-\mu^+\mu^-$  for a similar sample size; thus, only the first order term ( $\alpha_{\text{DIP}}$ ) is relevant in this analysis. We measure  $\alpha_{\text{DIP}}^{\text{eff}} = -1.1 \pm 0.6(\text{stat})$ . This value is in agreement with our measured value of  $\alpha_{K^*}^{\text{eff}}$  since the relation between the two is simply  $\alpha_{\text{DIP}} \approx -1 + 2.8\alpha_{K^*}$  (obtained by a Taylor expansion of the BMS form factor).

A first order Taylor expansion of the  $K_L \rightarrow e^+e^-e^+e^-$  form factors yields a generic linear form factor [ $1 + \alpha_{\text{Taylor}}(x_1 + x_2)$ ], with  $\alpha_{\text{Taylor}} \approx (0.42\text{--}1.2)\alpha_{K^*} \approx -\alpha_{\text{DIP}}/2.4$ . We measure an effective parameter  $\alpha_{\text{Taylor}}^{\text{eff}} = 0.5 \pm 0.3(\text{stat})$ .

We measure the branching ratio of  $K_L \rightarrow e^+e^-e^+e^-$  by normalizing to a sample of 49 809  $K_L \rightarrow \pi^0\pi_D^0\pi_D^0$  decays ( $\pi_D^0$  refers to the Dalitz decay  $\pi^0 \rightarrow e^+e^-\gamma$ ). These events were collected using the same trigger as for  $K_L \rightarrow e^+e^-e^+e^-$ . Off-line selection criteria are similar to those used in the  $K_L \rightarrow e^+e^-e^+e^-$  analysis. We require four photons, the eight-body ( $e^+e^-e^+e^-\gamma\gamma\gamma\gamma$ )  $P_T^2$  to be less than  $800 (\text{MeV}/c)^2$  and  $|M_{e^+e^-e^+e^-\gamma\gamma\gamma\gamma} - M_{K^0}|$  to be less than  $20 \text{ MeV}/c^2$ . The minimum track separation at the most upstream drift chamber is required to be greater than 1 mm to reduce conversion background, such as  $K_L \rightarrow \pi^0\pi_D^0\pi_D^0$  with a photon from one of the non-Dalitz  $\pi^0$ 's converting to  $e^+e^-$ . The background to  $K_L \rightarrow \pi^0\pi_D^0\pi_D^0$  from photon conversions in detector material is estimated to be  $844 \pm 66$  events. Another background is  $K_L \rightarrow \pi^0\pi^0\pi_{DD}^0$  ( $\pi_{DD}^0$  refers to the double Dalitz decay  $\pi^0 \rightarrow e^+e^-e^+e^-$ ) since both have the same eight-particle final state. There are 24 possible combinations of  $e^\pm$ 's and  $\gamma$ 's that yield  $K_L \rightarrow \pi^0\pi_D^0\pi_D^0$  and three combinations that yield  $K_L \rightarrow \pi^0\pi^0\pi_{DD}^0$ . We separate the two modes based on the best  $\chi^2$  for the corresponding  $\pi^0$  decay hypothesis. In addition, we require  $M_{\gamma\gamma}$  to be between  $127.5\text{--}142.5 \text{ MeV}/c^2$ ,  $M_{e^+e^-}$  between  $127.5\text{--}142.5 \text{ MeV}/c^2$ , and we exclude the region of  $M_{e^+e^-e^+e^-}$  between  $127.5\text{--}142.5 \text{ MeV}/c^2$ . The number

of  $K_L \rightarrow \pi^0 \pi^0 \pi_{DD}^0$  background events is estimated to be  $21 \pm 3$  events. With these selection criteria, we estimate a total of 865 background events for the normalization mode  $K_L \rightarrow \pi^0 \pi_D^0 \pi_D^0$ .

The  $K_L \rightarrow e^+ e^- e^+ e^-$  Monte Carlo, used to estimate detector acceptance, incorporates the BMS form factor with  $\alpha_{K^*}^{\text{eff}} = -0.14$ , our measured value. For the normalization mode  $K_L \rightarrow \pi^0 \pi_D^0 \pi_D^0$ , a QED calculation of radiative corrections exists in literature [13] and is included in our simulation. We measure the branching ratio of  $K_L \rightarrow e^+ e^- e^+ e^-$  to be  $[3.72 \pm 0.18(\text{stat}) \pm 0.10(\text{syst}) \pm 0.20(\text{norm})] \times 10^{-8}$  (“norm” refers to the measurement uncertainty in the normalization branching ratio [3]), consistent with the theoretical prediction  $3.65 \times 10^{-8}$  [2] and the most precise published experimental result  $[3.96 \pm 0.78(\text{stat}) \pm 0.32(\text{syst})] \times 10^{-8}$  [4]. Varying  $\alpha_{K^*}^{\text{eff}}$  by our measured uncertainty of  $\pm 0.23$  yields a systematic uncertainty in the  $K_L \rightarrow e^+ e^- e^+ e^-$  branching ratio of 0.9%. The addition of final state bremsstrahlung in the Monte Carlo simulation does not affect this result significantly. We assign a 1.1% error due to limited Monte Carlo statistics and a 2.2% error due to uncertainties in detector acceptance, which is dominated by the uncertainty in the track reconstruction efficiency. The 5.5% uncertainty in the  $K_L \rightarrow \pi^0 \pi_D^0 \pi_D^0$  branching ratio [3] results in an additional systematic error. The combined systematic error is 6.1%. Our measurement of the ratio  $B(K_L \rightarrow e^+ e^- e^+ e^-)/B(\pi^0 \rightarrow e^+ e^- \gamma)^2 = [2.59 \pm 0.12(\text{stat}) \pm 0.07(\text{syst})] \times 10^{-4}$  is unaffected by the large uncertainty in the  $\pi_D^0$  branching ratio measurement.

We search for  $CP$  violation in  $K_L \rightarrow e^+ e^- e^+ e^-$  by studying the angle  $\phi$  between the planes of the two  $e^+ e^-$  pairs in the kaon rest frame. We fit the  $\phi$  distribution to [4]

$$\frac{d\Gamma(K_L \rightarrow e^+ e^- e^+ e^-)}{d\phi} \propto 1 + \beta_{CP} \cos(2\phi) + \gamma_{CP} \sin(2\phi), \quad (1)$$

$$\beta_{CP} = \frac{1 - |\epsilon r|^2}{1 + |\epsilon r|^2} B, \quad \gamma_{CP} = \frac{2 \text{Re}(\epsilon r)}{1 + |\epsilon r|^2} C,$$

where  $\epsilon$  is the  $CP$  violating mixing parameter and  $r$  (which is approximately unity) is the ratio of the amplitudes of  $K_1$  and  $K_2$  decaying to  $e^+ e^- e^+ e^-$ . Ignoring  $CP$  violation, i.e., neglecting  $\epsilon$ , Eq. (1) reduces to the Kroll-Wada formula [14], where the constant  $B$  is  $-(+)$ 0.20 for an odd(even)  $CP$  eigenstate. With the introduction of  $CP$  violation the coefficient  $\beta_{CP}$  of the  $\cos(2\phi)$  term differs from  $B$  and the  $\sin(2\phi)$  term,  $\gamma_{CP}$ , no longer vanishes. Unfortunately, there are no predictions for the constant  $C$ , and therefore for  $\gamma_{CP}$ .

We measure the  $CP$  parameters  $\beta_{CP}$  and  $\gamma_{CP}$  using the distribution of the angle  $\phi$ . For the purposes of this measurement, we choose the  $e^+ e^-$  pairing that minimizes the product of the two  $e^+ e^-$  invariant masses. In reality, both

pairings contribute to the matrix element since there are identical particles in the final state; the pairing we choose is the dominant contribution. To optimize simultaneously the detector resolution of  $\phi$  and the statistical error, we require the invariant masses of the  $e^+ e^-$  pairs,  $M_{ee1}$  and  $M_{ee2}$ , to be greater than  $8 \text{ MeV}/c^2$ , retaining 264 events. Our expectation for  $B$  becomes  $-0.25$  as a result of discarding low  $M_{ee}$  events. We measure  $\beta_{CP} = -0.23 \pm 0.09(\text{stat}) \pm 0.02(\text{syst})$  and  $\gamma_{CP} = -0.09 \pm 0.09(\text{stat}) \pm 0.02(\text{syst})$  after correcting the  $\phi$  distribution for detector acceptance (Fig. 4). We estimate a systematic error of 0.014 and 0.021 in  $\beta_{CP}$  and  $\gamma_{CP}$ , respectively, due to acceptance uncertainties and an error of 0.008 in both  $\beta_{CP}$  and  $\gamma_{CP}$  due to detector resolution. We also set a 90% confidence level (C.L.) limit of  $|\gamma_{CP}| < 0.21$ . These results are consistent with the hypothesis that the decay proceeds predominantly through the  $CP = -1$  ( $K_2$ ) state. These parameters are insensitive to the effective form factor and to the inclusion of final state bremsstrahlung in the Monte Carlo.

In summary, we observe 441  $K_L \rightarrow e^+ e^- e^+ e^-$  candidate events with an estimated background of 4.2 events. We measure  $B(K_L \rightarrow e^+ e^- e^+ e^-) = [3.72 \pm 0.18(\text{stat}) \pm 0.23(\text{syst})] \times 10^{-8}$ . We also study the form factor for the first time in  $K_L \rightarrow e^+ e^- e^+ e^-$ . Our measurements of  $\alpha_{K^*}^{\text{eff}}(\text{BMS}) = -0.14 \pm 0.16(\text{stat}) \pm 0.15(\text{syst})$ ,

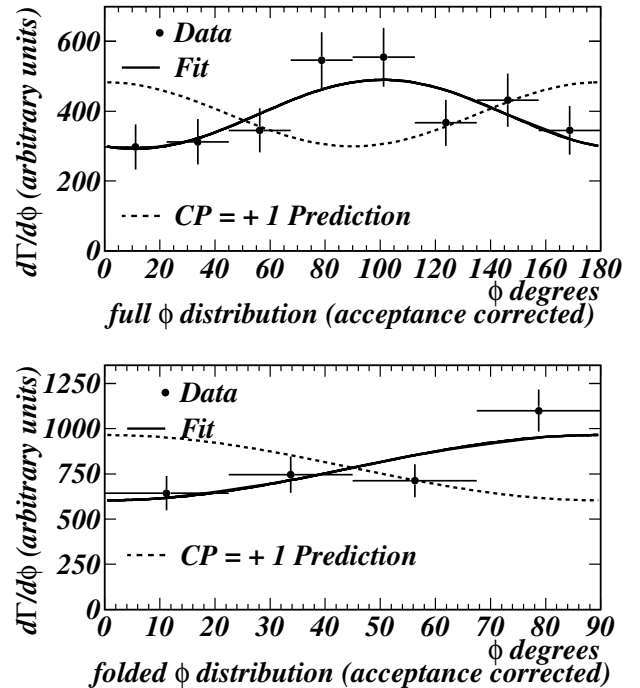


FIG. 4. The distribution of the angle  $\phi$  between the planes of the two  $e^+ e^-$  pairs. In the bottom panel, the  $\phi$  distribution from  $90^\circ$ – $180^\circ$  is folded into  $0^\circ$ – $90^\circ$ . We fit these distributions to Eq. (1) and measure  $\beta_{CP} = -0.23 \pm 0.09(\text{stat}) \pm 0.02(\text{syst})$  and  $\gamma_{CP} = -0.09 \pm 0.09(\text{stat}) \pm 0.02(\text{syst})$ . The dashed line shows the  $CP = +1$  ( $K_1$ ) prediction and further confirms that the decay proceeds predominantly through the  $CP = -1$  ( $K_2$ ) state.

$\alpha_{\text{DIP}}^{\text{eff}} = -1.1 \pm 0.6(\text{stat})$ , and  $\alpha_{\text{Taylor}}^{\text{eff}} = 0.5 \pm 0.3(\text{stat})$  describe the combined effects of a form factor and of radiative effects. We measure the  $CP$  parameters  $\beta_{CP} = -0.23 \pm 0.09(\text{stat}) \pm 0.02(\text{syst})$  and  $\gamma_{CP} = -0.09 \pm 0.09(\text{stat}) \pm 0.02(\text{syst})$  ( $M_{ee} > 8 \text{ MeV}/c^2$ ), thus limiting  $|\gamma_{CP}|$  to less than 0.21 at 90% C.L.

We gratefully acknowledge the support and effort of the Fermilab staff and the technical staffs of the participating institutions for their vital contributions. This work was supported in part by the U.S. Department of Energy, The National Science Foundation, and The Ministry of Education and Science of Japan.

---

\*To whom correspondence should be addressed.

Electronic address: evah@fnal.gov

†On leave from C.P.P.Marseille/C.N.R.S., Marseille, France.

- [1] G. Bélanger and C. Q. Geng, Phys. Rev. D **43**, 140 (1991).
- [2] T. Miyazaki and E. Takasugi, Phys. Rev. D **8**, 2051 (1973). With a correction to the interference term (see Ref. [4]).
- [3] Particle Data Group, D. E. Groom *et al.*, Eur. Phys. J. C **15**, 395 (2000).
- [4] P. Gu *et al.*, Phys. Rev. Lett. **72**, 3000 (1994).
- [5] J. Adams *et al.*, Phys. Rev. Lett. **80**, 4123 (1998).
- [6] E. Halkiadakis, Ph.D. thesis, Rutgers University, 2001.
- [7] E. D. Zimmerman, Nucl. Inst. Methods Phys. Res., Sect. A **426**, 229 (1999).
- [8] L. Bergström *et al.*, Phys. Lett. **131B**, 229 (1983). The evaluation of this form factor is based on information found in [3].
- [9] K. E. Ohl *et al.*, Phys. Rev. Lett. **65**, 1407 (1990).
- [10] A. Alavi-Harati *et al.*, Phys. Rev. Lett. **84**, 408 (2000).
- [11] V. Fanti *et al.*, Phys. Lett. B **458**, 553 (1999).
- [12] G. D'Ambrosio, G. Isidori, and J. Portolés, Phys. Lett. B **423**, 385 (1998). The evaluation of this form factor is based on information found in [3].
- [13] K. O. Mikaelian and J. Smith, Phys. Rev. D **5**, 1763 (1972).
- [14] N. M. Kroll and W. Wada, Phys. Rev. **98**, 1355 (1955).